



Indoor and Outdoor Spectroradiometer Intercomparison for Spectral Irradiance Measurement

A. Habte,¹ A. Andreas,¹ L. Ottoson,¹
C. Gueymard,² G. Fedor,³ S. Fowler,³
J. Peterson,⁴ E. Naranen,⁵ T. Kobashi,⁶
A. Akiyama,⁶ and S. Takagi⁶

¹ National Renewable Energy Laboratory

² Solar Consulting Services

³ Q-Lab Corporation

⁴ University of Oregon

⁵ Atlas Material Testing Technology, LLC

⁶ EKO Instruments, Inc.

**NREL is a national laboratory of the U.S. Department of Energy
Office of Energy Efficiency & Renewable Energy
Operated by the Alliance for Sustainable Energy, LLC**

This report is available at no cost from the National Renewable Energy Laboratory (NREL) at www.nrel.gov/publications.

Technical Report
NREL/TP-5D00-61476
May 2014

Contract No. DE-AC36-08GO28308

Indoor and Outdoor Spectroradiometer Intercomparison for Spectral Irradiance Measurement

A. Habte,¹ A. Andreas,¹ L. Ottoson,¹
C. Gueymard,² G. Fedor,³ S. Fowler,³
J. Peterson,⁴ E. Naranen,⁵ T. Kobashi,⁶
A. Akiyama,⁶ and S. Takagi⁶

¹ National Renewable Energy Laboratory

² Solar Consulting Services

³ Q-Lab Corporation

⁴ University of Oregon

⁵ Atlas Material Testing Technology, LLC

⁶ EKO Instruments, Inc.

Prepared under Task No. SS13.3513

**NREL is a national laboratory of the U.S. Department of Energy
Office of Energy Efficiency & Renewable Energy
Operated by the Alliance for Sustainable Energy, LLC**

This report is available at no cost from the National Renewable Energy Laboratory (NREL) at www.nrel.gov/publications.

NOTICE

This report was prepared as an account of work sponsored by an agency of the United States government. Neither the United States government nor any agency thereof, nor any of their employees, makes any warranty, express or implied, or assumes any legal liability or responsibility for the accuracy, completeness, or usefulness of any information, apparatus, product, or process disclosed, or represents that its use would not infringe privately owned rights. Reference herein to any specific commercial product, process, or service by trade name, trademark, manufacturer, or otherwise does not necessarily constitute or imply its endorsement, recommendation, or favoring by the United States government or any agency thereof. The views and opinions of authors expressed herein do not necessarily state or reflect those of the United States government or any agency thereof.

This report is available at no cost from the National Renewable Energy Laboratory (NREL) at www.nrel.gov/publications.

Available electronically at <http://www.osti.gov/scitech>

Available for a processing fee to U.S. Department of Energy and its contractors, in paper, from:

U.S. Department of Energy
Office of Scientific and Technical Information
P.O. Box 62
Oak Ridge, TN 37831-0062
phone: 865.576.8401
fax: 865.576.5728
email: <mailto:reports@adonis.osti.gov>

Available for sale to the public, in paper, from:

U.S. Department of Commerce
National Technical Information Service
5285 Port Royal Road
Springfield, VA 22161
phone: 800.553.6847
fax: 703.605.6900
email: orders@ntis.fedworld.gov
online ordering: <http://www.ntis.gov/help/ordermethods.aspx>

Cover Photos: (left to right) photo by Pat Corkery, NREL 16416, photo from SunEdison, NREL 17423, photo by Pat Corkery, NREL 16560, photo by Dennis Schroeder, NREL 17613, photo by Dean Armstrong, NREL 17436, photo by Pat Corkery, NREL 17721.



Printed on paper containing at least 50% wastepaper, including 10% post consumer waste.

Acknowledgments

The spectral irradiance intercomparison was a collective effort made by participating laboratories EKO instruments, Inc.; Q-Lab Corporation; ATLAS Material Testing Technology, LLC; the University of Oregon's Department of Physics; and Solar Consulting Services. We would like to thank Daryl Myers, as well as Peter Gotseff and Manajit Sengupta of the National Renewable Energy Laboratory for their critical reviews and invaluable suggestions.

List of Acronyms

ASTM	American Society for Testing and Materials
IEC	International Electrotechnical Commission
ISO	International Organization for Standardization
MBE	mean bias error
NIST	National Institute of Standards and Technology
NREL	National Renewable Energy Laboratory
RMSE	root mean square error
SMARTS	Simple Model of the Atmospheric Radiative Transfer of Sunshine
SRRL	Solar Radiation Research Laboratory

Executive Summary

A global spectral irradiance intercomparison using spectroradiometers was organized by the National Renewable Energy Laboratory's (NREL's) Solar Radiation Research Laboratory. The intercomparison was performed both indoors and outdoors on September 17, 2013. Five laboratories participated in the intercomparison using 10 spectroradiometers. A coordinated measurement setup and a common platform were employed to compare spectral irradiances under both indoor and outdoor conditions. The intercomparison was aimed at understanding the performance of the different spectroradiometers and sharing knowledge in making spectral irradiance measurements. At NREL's Optical Metrology Laboratory, the intercomparison is part of an internal performance-based quality-control check to monitor the legitimacy of a measurement and calibration undertaken by a laboratory to demonstrate compliance with International Standards Organization/International Electrotechnical Commission (ISO/IEC) 17025 accreditation requirements.

The indoor performance comparison showed that all of the participating spectroradiometers had satisfactory statistical results (± 1) compared to the NREL reference instrument. However, each laboratory's instruments behaves differently with respect to the statistical limit, and such differences could be related to various reasons—for example, differing calibration setups from one laboratory to another, differing environmental conditions inside laboratories, whether a primary or secondary spectral irradiance calibration lamp was used for the calibration, instrument age, and the amount of time since the last calibration.

The outdoor intercomparison showed up to $\pm 10\%$ deviation relative to the average spectral irradiance measured by the participating spectroradiometers. Differing scan rates, sizes of the entrance optics, or fast-changing atmospheric conditions could be reasons for such deviations. Mean bias error (MBE) and root mean square error (RMSE) were calculated representing average differences from the three outdoor runs and results from the aggregation of hundred-wavelength bins. Almost all instruments were within $+10\%$ MBE and 10% RMSE.

Simulations using the Simple Model of the Atmospheric Radiative Transfer of Sunshine (SMARTS) were applied to the outdoor intercomparison as an explanatory tool and to understand how well the SMARTS-modeled spectra compare to various types of spectroradiometers considering the model's spectral resolution compared to the spectroradiometers under scrutiny. Running the smoothing postprocessor of the SMARTS model was therefore necessary to downgrade the resolution of its spectra and make them match that of any specific instrument based on the shape of its passband (e.g., Gaussian), its width (as measured by the full width at half maximum), and its wavelength step (e.g., 5 nm). The SMARTS model in the outdoor intercomparison provides relevant information when predicting clear-sky solar spectral irradiance under varying atmospheric conditions. The output from the model compared well to the outdoor spectroradiometers' spectral irradiance outputs, and the differences were within the margin of error.

Table of Contents

List of Figures	vii
List of Tables	vii
1 Introduction.....	1
2 Objective.....	2
3 Method and Instrumentation	3
4 Results and Discussions	6
4.1 Indoor Intercomparison.....	6
4.2 Outdoor Intercomparison	9
4.2.1 Experimental Conditions.....	9
4.2.2 Experimental Results	11
4.2.3 Modeled Spectra	13
4.2.4 Scanning Speed and Cloud Detection	15
4.2.5 Performance Analysis	16
4.2.6 Comparison to a Single Instrument.....	18
5 Summary	19
6 References	20

List of Figures

Figure 1. Schematic layout of the relative position of each participating spectroradiometer.....	4
Figure 2. Performance statistics results using Equation 1	7
Figure 3. Plots showing indoor differences/ratios performed using the NIST FEL lamp.....	8
Figure 4. (Left) Broadband data for global horizontal irradiance, direct normal irradiance, diffuse horizontal irradiance, and solar zenith angle (secondary axis). The yellow box indicates the outdoor measurement period. (Top right) Picture taken from SRRL showing the frequent photochemical smog over Denver, Colorado. <i>Photo by Mike Dooraghi and Tom Stoffel</i> (Bottom right) Picture from the SRRL TSI 880 sky imager showing the small and fast cumulus cloud that affected measurements.....	10
Figure 5. One-minute broadband data for global horizontal irradiance and direct normal irradiance during the experimental period showing the rapid variations in both signals, the decreasing trend in direct normal irradiance after 11:00 LST, and the impact of the passing cumulus cloud at solar noon.	10
Figure 6. A fast-response instrument (NREL-5) showing a dip in spectral measurement due to a small and fast-moving cumulus cloud at approximately 11:55:11 LST. Spectral measurements before and after the 11:55:11 measurements do not show the dip.....	11
Figure 7. The three outdoor runs, from top to bottom, showing the (left) spectral irradiance plot for each participating spectroradiometer and SMARTS model spectral irradiance output and (right) ratio using the average spectrum from the participating spectroradiometers	13
Figure 8. Three spectral irradiance results using the SMARTS model. Input values were selected using the applicable period of run.....	15
Figure 9. MBE in percent (from Table 2) for various spectral ranges	17
Figure 10. RMSE in percent (from Table 2) for various spectral ranges	17
Figure 11. Spectral irradiance data differences for the three runs.....	18

List of Tables

Table 1. Participating Spectroradiometer Characteristics.....	5
Table 2. Average MBE and RMSE in Percent	16

1 Introduction

In September 2013, an intercomparison of spectroradiometers measuring global horizontal spectral irradiance measurements was performed. Five calibration laboratories participated in this intercomparison, which was held at the National Renewable Energy Laboratory's (NREL's) Solar Radiation Research Laboratory (SRRL). The intercomparison was performed to understand the reliability of the spectroradiometer systems, compare results from different instruments, and share knowledge about the process of making spectral irradiance measurements using various types of spectroradiometers. The intercomparison is part of an internal performance-based quality-control check to monitor the legitimacy of a measurement and calibration undertaken by a laboratory (e.g., NREL's Optical Metrology Laboratory) to demonstrate compliance with International Standards Organization/International Electrotechnical Commission (ISO/IEC) 17025 accreditation requirements. Further, participating in an intercomparison provides technical competency for accredited laboratories.

Similar intercomparisons of spectroradiometers for solar applications have been conducted in other countries (see, for example, Martinez-Lozano et al. 2003 and Galleano et al. 2013), and their results have been beneficial to improving laboratories' specialized spectral measurement capabilities, reducing metrological sources of errors, and increasing result comparability despite differing equipment. In the United States, interagency intercomparisons had been conducted only for ultraviolet spectroradiometers (Lantz et al. 2002; Thompson et al. 1997), thus the present study was the first of its kind.

NREL's Optical Metrology Laboratory coordinated the indoor and outdoor comparisons presented in this document. In addition to NREL, EKO instruments, Inc.; Q-Lab Corporation; ATLAS Material Testing Technology, LLC; and the University of Oregon's Department of Physics participated in the intercomparison. The outdoor intercomparison was conducted on September 17, 2013, at approximately solar noon between 11:00 LST and 13:30 LST. That time period was selected to avoid large variations in solar zenith angle and irradiance and also to reduce cosine effects in global horizontal spectral irradiance measurements due to the instruments' entrance optics. Three runs were made during the specified time period. The solar irradiance (sun) was used as the source for the comparison. Additionally, an indoor comparison was made at NREL's Optical Metrology Laboratory using a National Institute of Standards and Technology (NIST) FEL lamp.

This report summarizes the comparison results made over the spectral range from 380 nm to 1,100 nm for global spectral irradiance measurements using different spectroradiometers. Because the participating spectroradiometers had differing wavelength ranges, we had to limit the comparison to a common specified wavelength range to obtain valid results overall.

2 Objective

An intercomparison is an essential method for evaluating the performance of spectroradiometers, comparing results, and objectively verifying the technical competence of laboratories. To ensure that all data collection, processing, and analyses are consistent, a common procedure was established for this intercomparison. NREL facilitated the comparison as well as the presentation of the results and sharing of information among participants. This report provides an unbiased assessment of the intercomparison under a mutually agreed framework. The requirements for this framework included that (1) the process and analysis of the data from the individual laboratories is to be kept confidential; (2) all participating spectroradiometers should have the same measurement setup, such as the outdoor measurement height and indoor measurement setup; (3) the start and end time of the outdoor measurement should be determined using the slowest scanning instrument; and (4) the comparison should be made using the common wavelength range from the participating spectroradiometers (380 nm to 1,100 nm).

3 Method and Instrumentation

The measurement was conducted indoors and outdoors using multiple spectroradiometers under controlled laboratory conditions and under clear-sky conditions at approximately solar noon, respectively. This event took place during a single day, on September 17, 2013, close to the fall equinox, and during a period when clear conditions normally prevail at SRRL. Prior to the comparison, each instrument was calibrated either by the participant laboratory or by a recognized outside laboratory. In this report, no major effort was made to harmonize the inherent differences among instruments in terms of differing calibration date, instrument integration/measurement time, bandwidth size, or wavelength interval. The postprocessing of the indoor and outdoor comparisons was made at 5-nm intervals. Data from instruments with a higher resolution (less than 5 nm) were linearly interpolated to 5 nm before the indoor and outdoor data sets were compared.

The instrument characteristics are shown in Table 1. The instruments were operated by personnel representing each laboratory for the three outdoor comparison runs. Further, all spectroradiometers sat on the same height of measurement to avoid any occlusion of one instrument by another from the entire sky vault (180°). This means that all spheres, cosine receptors, and diffusers sat 25 cm above the sitting surface. A run is determined by the duration of time that the slowest instrument takes to finish its scan. For the outdoor measurements, each instrument had a specific time interval within which to finish a measurement scan for the specified wavelength range. Therefore, instruments with faster time scans continued to measure until the slowest instrument finished its scan. Then, to obtain a comparable data set, the multiple files from the fast instruments were averaged to obtain one single result file with which the comparison analysis was performed for each run. All of the outdoor measurements were made within ± 1.5 hour from solar noon, thus determining a period during which the sun's zenith angle was lower than 43.5° .

The indoor comparisons were performed using NREL's FEL tungsten lamp (F407), which NREL does not use to calibrate spectroradiometers. The intent of the indoor comparison was to identify subtle shifts and trends that would be clearly seen in each spectroradiometer measurement due to factors such as differing calibration laboratories, methods of calibration setup, or type of lamp used to calibrate the instruments. Therefore, one spectroradiometer from each calibration laboratory was selected. During the indoor comparison, each instrument setup was the same, and data collection was made by the owner of each instrument. The NREL-1 system was considered a reference instrument for the indoor comparison because it is reliable, repeatable, and has less uncertainty than the other NREL spectroradiometers that participated in this intercomparison.

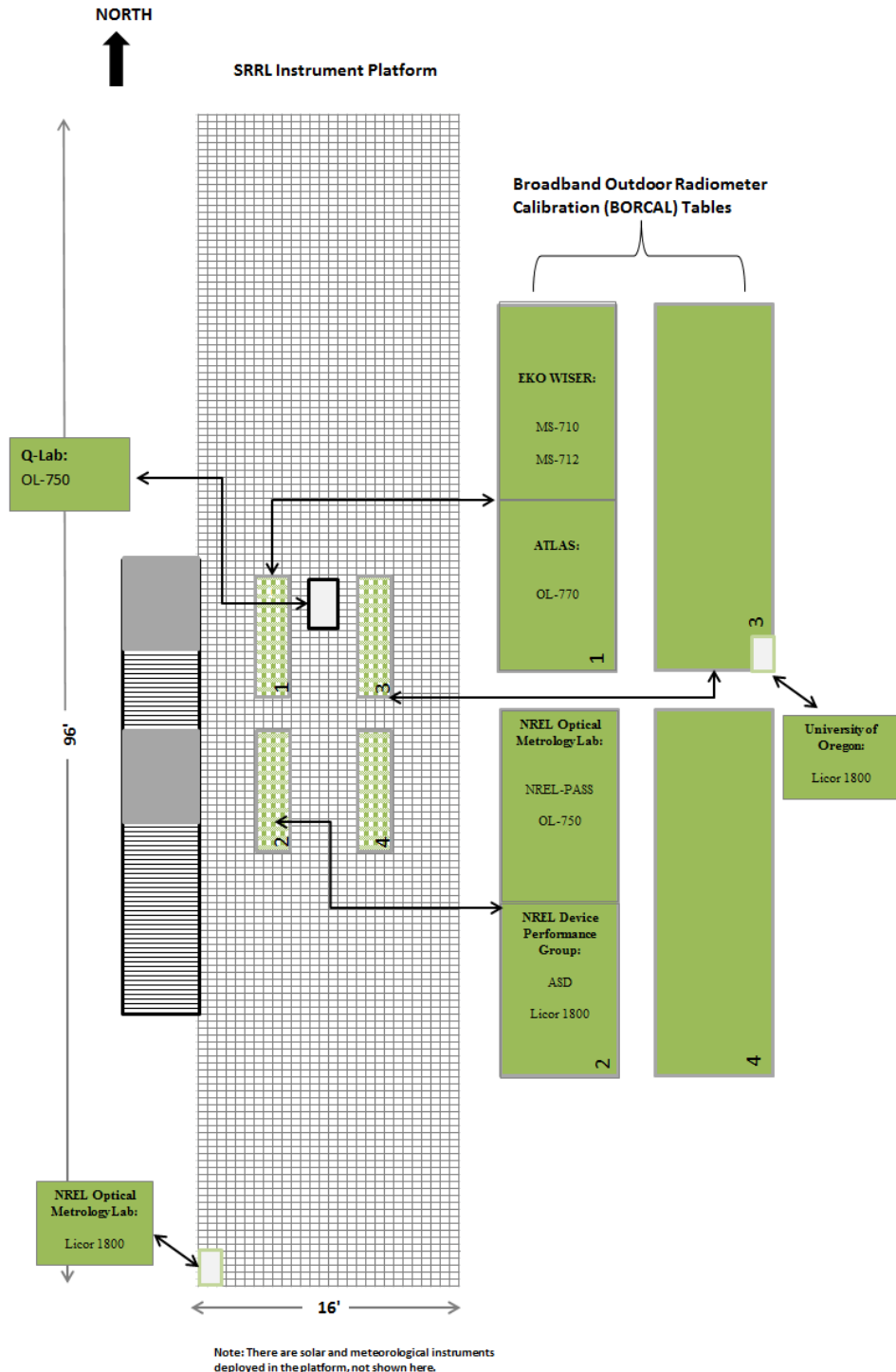


Figure 1. Schematic layout of the relative position of each participating spectroradiometer

During the analysis, the participants' identity remained undisclosed, thus guaranteeing data confidentiality. Each organization is identified here using only a generic name (Lab-1, Lab-2, etc.). However, each participant was privately given their respective laboratory number so that they could access their own results.

Table 1. Participating Spectroradiometer Characteristics

Organization	Type of Spectroradiometer	Wavelength Range (nm)	Entrance Optics	Calibration Standard/Lamp	Detector	Calibrating Laboratory and Date of Calibration
NREL (SRRL)	OL750	280–2,400	Integrating sphere (6-inch)	NIST FEL Lamp F655 ASTM G138	Silicon/Ge/Pbs	NREL Optical Metrology Laboratory September 16, 2013
EKO Instruments	WISER: MS-710/MS-712 (Polychromator)	350–1,700	Dome/ diffuser	Optronics FEL Lamp ASTM G138	MS710: Silicon diode array/MS712: InGaAs diode array	Optronics December 20, 2012
NREL (SRRL)	LI-1800	380–1,100	Cosine receptor	NIST FEL Lamp F655 ASTM G138	Silicon	NREL Optical Metrology Laboratory April 15, 2013
Q-Lab	OL750/ Double Monochromator	280–1,100	Integrating sphere (6-inch)	Optronics FEL Lamp ASTM G138	Silicon	Gooch & Housego, traceable to NIST May 20, 2013
NREL (Device Performance Group)	ASD	350–2,400	Integrating sphere (4-inch, with dome)	NIST FEL Lamp F655 ASTM G138	Silicon diode array/InGaAs high-speed rotating grating/Extended infrared InGaAs high-speed rotating grating	NREL Optical Metrology Laboratory June 11, 2013
NREL (Device Performance Group)	LI-1800 (with NREL temperature controller)	380–1,100	Cosine receptor	NIST FEL Lamp F655 ASTM G138	Silicon	NREL Optical Metrology Laboratory June 13, 2013
NREL (SRRL)	Pulse Analysis Spectroradiometer System (PASS)	280–1,720	Integrating sphere (6-inch)	NIST FEL Lamp F655 ASTM G138	Silicon/InGaAs	NREL Optical Metrology Laboratory September 16, 2013
ATLAS	OL770 CCD Array	380–1,100	Integrating sphere (2-inch)	OL752-10 Plug-in Standard ASTM G138	Silicon diode array	ATLAS September 4, 2013
University of Oregon	LI-1800 (with University of Oregon temperature controller)	380–1,100	Cosine receptor	LI-COR 1800-02 Optical Radiation Calibrator (ORC) ASTM G138	Silicon	LI-COR, traceable to NIST September 29, 2011

4 Results and Discussions

4.1 Indoor Intercomparison

As mentioned above, the indoor comparison was performed using NREL's FEL tungsten lamp (F407). This lamp was selected for the comparison because it had less than 37 hours of usage, which is less than the 50 hours of use recommended by NIST, and also demonstrated good repeatability through time. Further, a statistical procedure was conducted to achieve a reasonable comparison result. The E_n performance statistics was selected, according to ISO/IEC 17043:2010 (*Conformity assessment—General requirements for proficiency testing*). Participants provided the estimated uncertainty value for spectral irradiance measurements using their spectroradiometer. To simplify the statistical comparison using the performance statistics method, the spectral irradiance data from the participating laboratories' spectroradiometers and the NREL reference spectroradiometer were integrated to seven 100-nm bins: 380 nm–400 nm, 400 nm–500 nm, 500 nm–600 nm, 600 nm–700 nm, 700 nm–800 nm, 800 nm–900 nm, 900 nm–1,000 nm, 1,000 nm–1,100 nm.

The performance statistic is defined as

$$E_n = \frac{M_{LABn} + M_{REF}}{\sqrt{(U_{LABn} * M_{LABn})^2 + (U_{REF} * M_{REF})^2}} \quad (1)$$

where E_n is normalized error (unitless) and U_{LABn} and U_{REF} are the reported calibration uncertainty in percent for the participating spectroradiometers of each laboratory and the NREL reference spectroradiometer, respectively. M_{LABn} represents the integrated measurements from participating organizations (LAB₁, LAB₂, LAB₃, etc.) in W/m², and M_{REF} is the integrated measurement data from the reference instrument (NREL-1) in W/m².

The performance statistics comparison (based on Equation 1) used integrated values in 100-nm bins, i.e., between 380 nm and 1,100 nm. Prior to the integration of the data, all data sets from the participating laboratories were interpolated to 5-nm intervals to obtain comparable data sets. Typically, the reported uncertainty from each participant is based on a 95% level of confidence. The observed deviation of E_n in Equation 1 involves the establishment of acceptable limits of ± 1 . Each reported limit is then determined to be either satisfactory (i.e., within the designated performance limit) or unsatisfactory (outside of the designated limit).

The results presented in this section contain all the necessary corrections using the calibration information for each spectroradiometer. Prior to the intercomparison, each participating instrument was calibrated by the participant in their own calibration facility/arrangement. Figure 2 and Figure 3 demonstrate the performance of each participating spectroradiometer relative to the NREL-1 system using the E_n statistic from Equation 1.

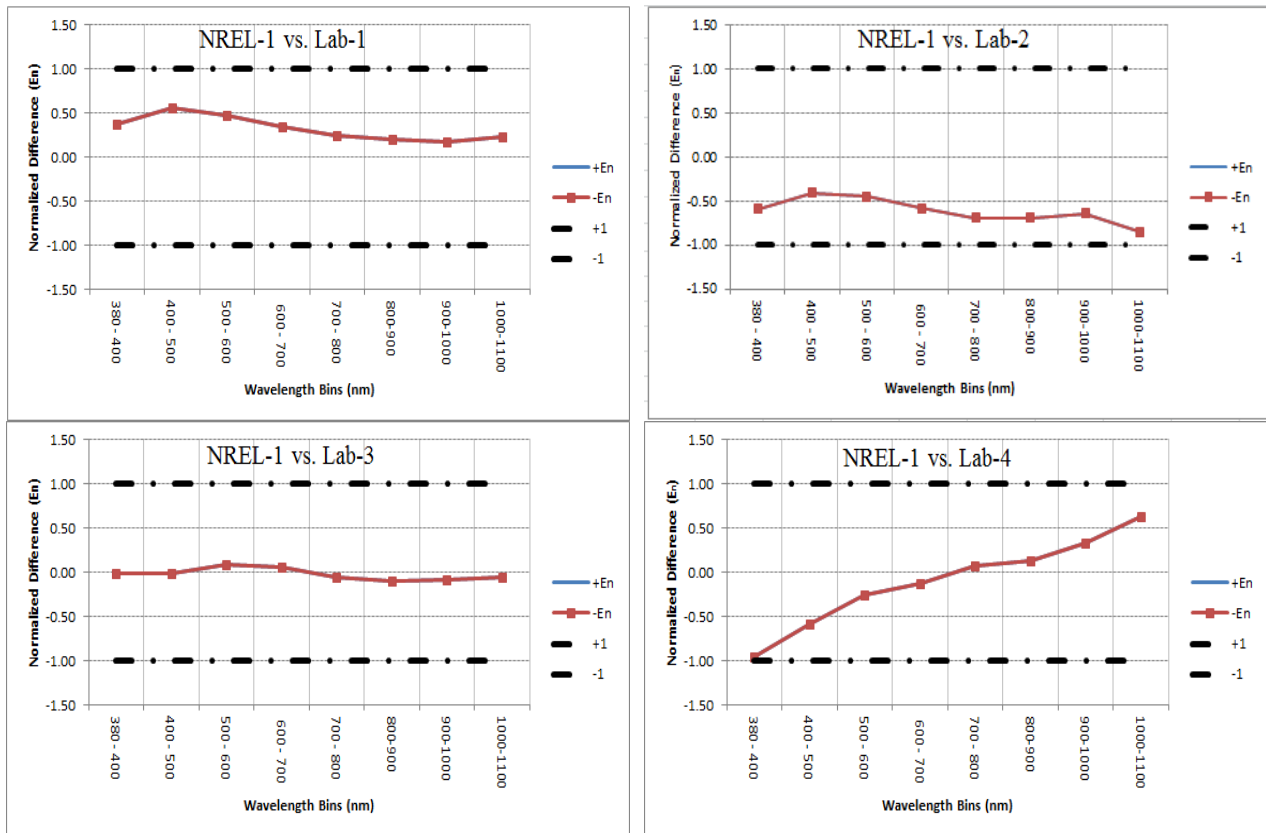


Figure 2. Performance statistics results using Equation 1

All laboratories reported satisfactory results for integrated irradiances for all the 100-nm intervals between 380 nm and 1,100 nm (Figure 2). However, it was observed that each laboratory's spectroradiometer showed different signatures in their performance statistic E_n . This could be a result of differences in calibration procedures, differing calibration setups from one laboratory to another, differing environmental conditions inside laboratories, whether a primary or secondary spectral irradiance calibration lamp was used for the calibrations, instrument age, and time elapsed since the last calibration, among others. It is also important to emphasize that the calibration uncertainty provided by each participating laboratory affects the determination of whether the performance statistic for their instrument is satisfactory (Equation 1). Lower reported calibration uncertainties could trigger higher or lower E_n values (even outside the limit of ± 1), which would push the participating laboratory into an unsatisfactory category.

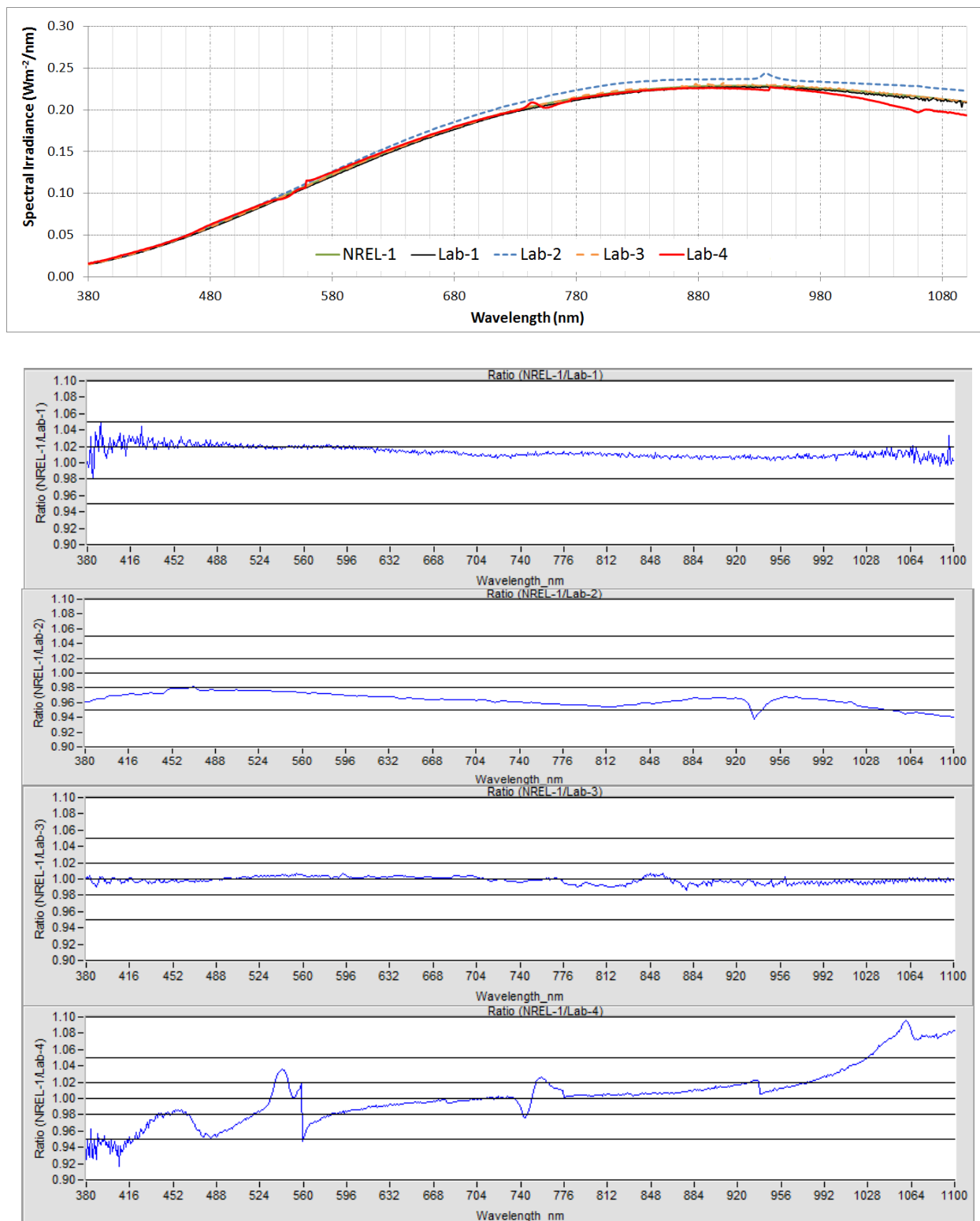


Figure 3. Plots showing indoor differences/ratios performed using the NIST FEL lamp

The top plot in Figure 3 shows the spectral irradiance in $\text{Wm}^{-2} \text{ nm}^{-1}$ versus wavelength (nm), whereas the bottom four plots provide the spectral irradiance ratios relative to the NREL-1 instrument. These ratios display significant differences from one instrument to another, with Lab-3 showing the closest similarity to the NREL-1 measurements and Lab-4 showing significant differences at specific wavelengths. Lab-1 values are persistently lower than NREL-1, whereas Lab-2 values are persistently higher. These ratios do not take into account the reported calibration uncertainty included in the proficiency test calculation of Figure 2.

4.2 Outdoor Intercomparison

4.2.1 Experimental Conditions

As mentioned above, the selection of the solar noon period has significant advantages because there is a reduction in inadvertent sources of errors and irradiance variations are limited during the measurements, especially when slow scanning instruments are used.

During the outdoor event, clear-sky conditions prevailed, except for a very short period (a few seconds) at solar noon, during which a small and fast-moving cumulus cloud obscured the sun. Further, as is shown in the broadband irradiance records from the main SRRL pyrheliometers and pyranometers (Figure 4 and Figure 5), there were slight and rapid irradiance perturbations around solar noon. These are typical circumstances at SRRL. They can be related to the location of SRRL on top of a mesa, which is thus affected by turbulent upslope flows of pollution aerosols and transients during the rapid lifting of the mixing layer during daytime (Gueymard 2011) and, to some extent, to the frequent photochemical smog conditions over the whole Denver agglomeration.

Rapidly changing atmospheric conditions have a direct effect on the spectral irradiance sensed by all spectroradiometers, more particularly those that have a slow scanning mechanism. Differing scan rates or sizes of the entrance optics can also impact the instrument-to-instrument response variability in fast-changing atmospheric conditions. From the results shown in Figure 5, it appears that during the measurement period global horizontal irradiance first increased from 833 W/m^2 at 11:00 LST to a daily maximum of 863 W/m^2 at 12:00 LST then decreased to 784 W/m^2 at 13:30 LST. These variations are normal for that season but may present a challenge for measurements carried out with instruments having very slow scanning mechanisms. Using the test day conditions, for instance, a natural variation of up to $\pm 5\%$ in global irradiance would typically occur during a 45-min scan. This natural variation adds to the uncertainty of the measurement itself, which has a similar magnitude. A possible way to limit this issue would be to use such instruments during the summer solstice period, when the solar zenith angle, and thus global horizontal irradiance, varies less during the noon hours. Clear-sky conditions, however, are not as frequent during that period as they are in September.

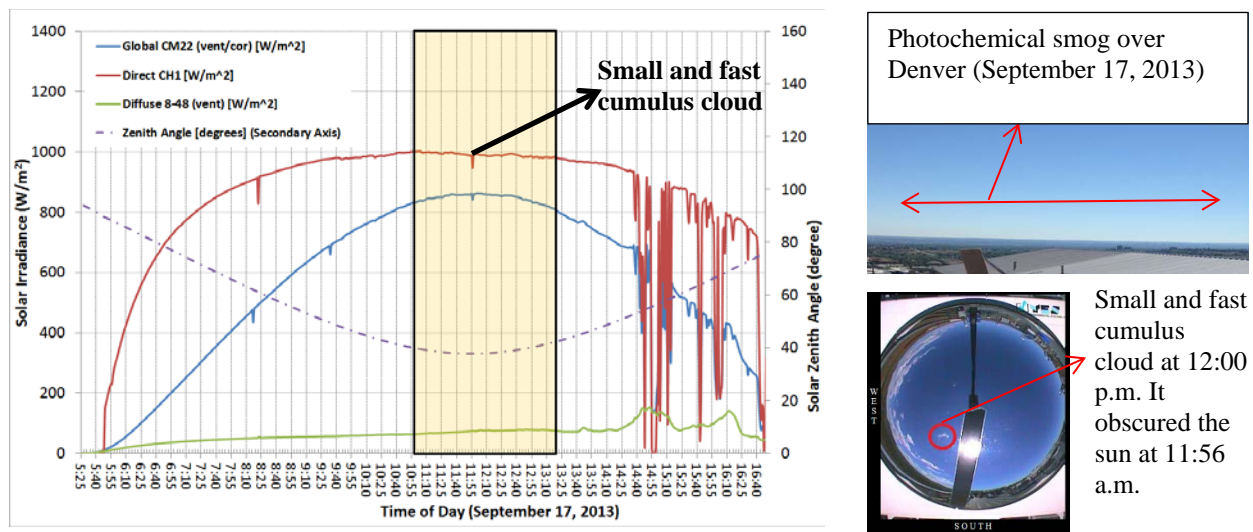


Figure 4. (Left) Broadband data for global horizontal irradiance, direct normal irradiance, diffuse horizontal irradiance, and solar zenith angle (secondary axis). The yellow box indicates the outdoor measurement period. (**Top right**) Picture taken from SRRL showing the frequent photochemical smog over Denver, Colorado. *Photo by Mike Dooraghi and Tom Stoffel* (**Bottom right**) Picture from the SRRL TSI 880 sky imager showing the small and fast cumulus cloud that affected measurements.

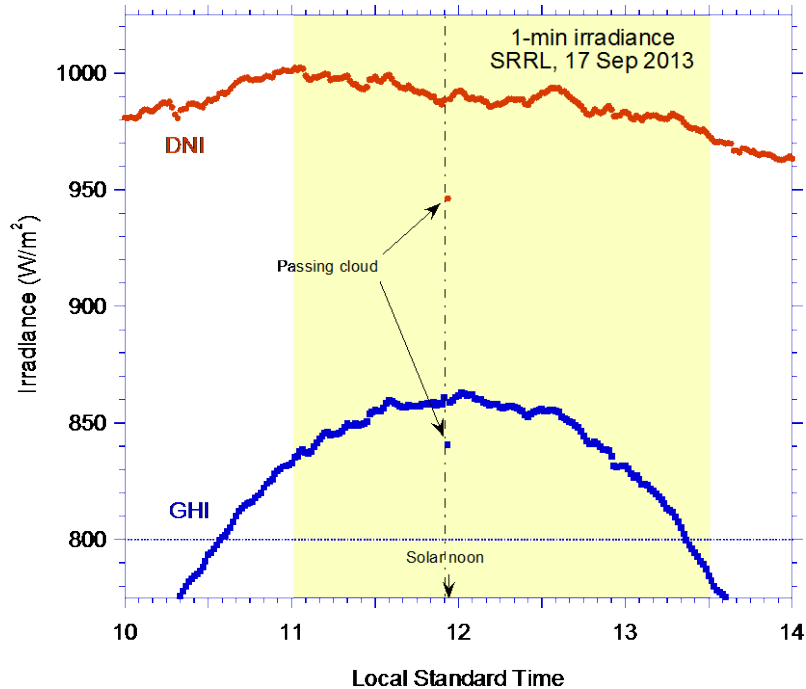


Figure 5. One-minute broadband data for global horizontal irradiance and direct normal irradiance during the experimental period showing the rapid variations in both signals, the decreasing trend in direct normal irradiance after 11:00 LST, and the impact of the passing cumulus cloud at solar noon.

4.2.2 Experimental Results

Two of the NREL spectroradiometers collected data at 5-nm intervals. Therefore, to obtain comparable results, the outdoor data analysis was performed at 5-nm intervals for all instruments. A linear interpolation method was applied to data sets obtained from the instruments that have a higher resolution. Further, the time used for each measurement run was determined by the time taken by the slowest instrument to finish its scan, i.e., approximately 45 minutes. The data from the faster instruments was averaged to perform the analysis. These values were obtained from the spectral irradiance measurement by the spectroradiometers in the range of 380 nm to 1,100 nm. An average spectral irradiance was calculated for each wavelength. The measured data from each spectroradiometer, as well as the modeled data from the Simple Model of the Atmospheric Radiative Transfer of Sunshine (SMARTS) code (see details in Section 4.2.3), was divided by the average values calculated from all *measured* data. Aside from spectral regions corresponding to sharp absorption bands, a fast-moving cloud (Figure 6), or spikes detected in one instrument due to unknown conditions, the relative difference among the instruments was less than 10% (Figure 7 (right)).

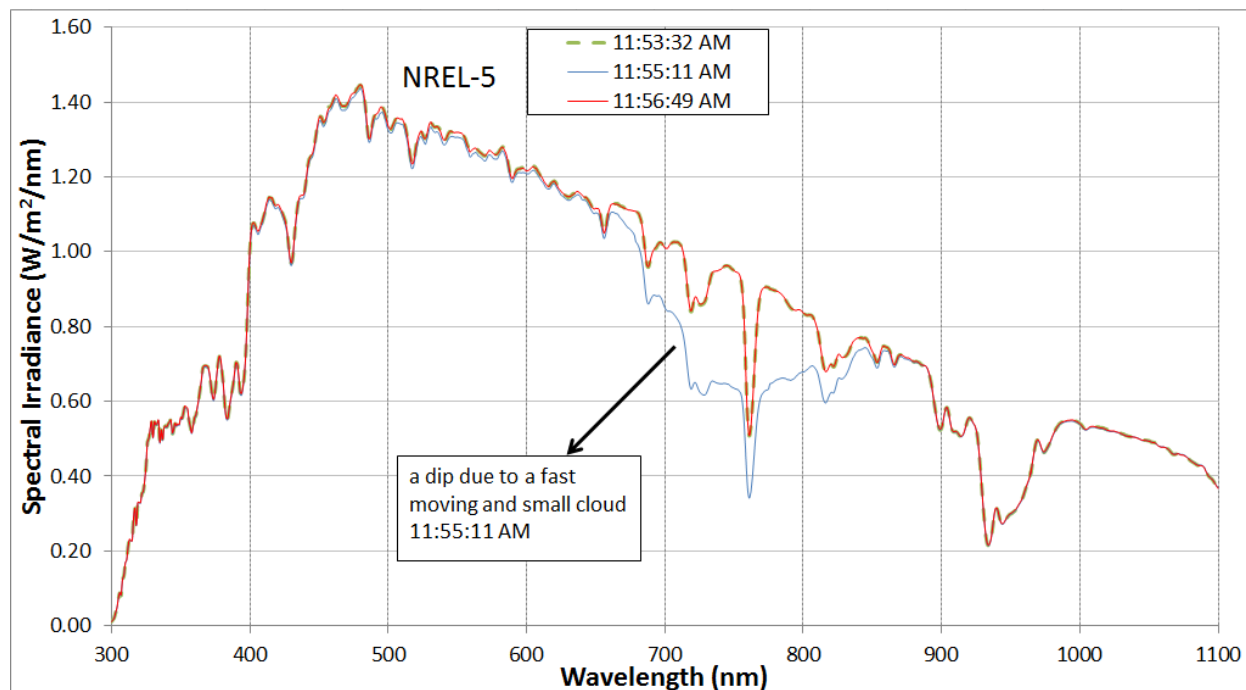


Figure 6. A fast-response instrument (NREL-5) showing a dip in spectral measurement due to a small and fast-moving cumulus cloud at approximately 11:55:11 LST. Spectral measurements before and after the 11:55:11 measurements do not show the dip.

The solar noon for September 17, 2013, occurred at approximately 11:54:30 LST, coinciding almost exactly with the passage of the noted cumulus cloud (Figure 4, Figure 5, and Figure 6). Except for such anomalous conditions, runs conducted close to solar noon are expected to yield lower differences in results than at any other time of the day. Indeed, the second run period, which was very close to solar noon, demonstrated relatively smaller differences. That second run had comparatively less air mass because of the smallest solar zenith angles of the day, as well as less variations in global horizontal irradiance during scan times.

The 380-nm to 400-nm and 1,000-nm to 1,100-nm spectral bands showed relatively higher differences compared to the rest of the spectrum. The relative higher percent difference of the former band could be related to the lower performance of most spectroradiometers in the ultraviolet region coupled with the higher uncertainty in the output of calibration lamps. The latter range (in the near infrared) could be related to the temperature dependence of the silicon detectors. In particular, out of the three LI-COR 1800s, one was not equipped with a temperature controller during the intercomparison. Moreover, one of the temperature-controlled LI-COR 1800s may have been calibrated at a different temperature than what was used during the intercomparison. In any case, the larger uncertainty of that instrument below 400 nm and above 900 nm has previously been described in the literature (Cachorro et al. 2009; Myers 1989).

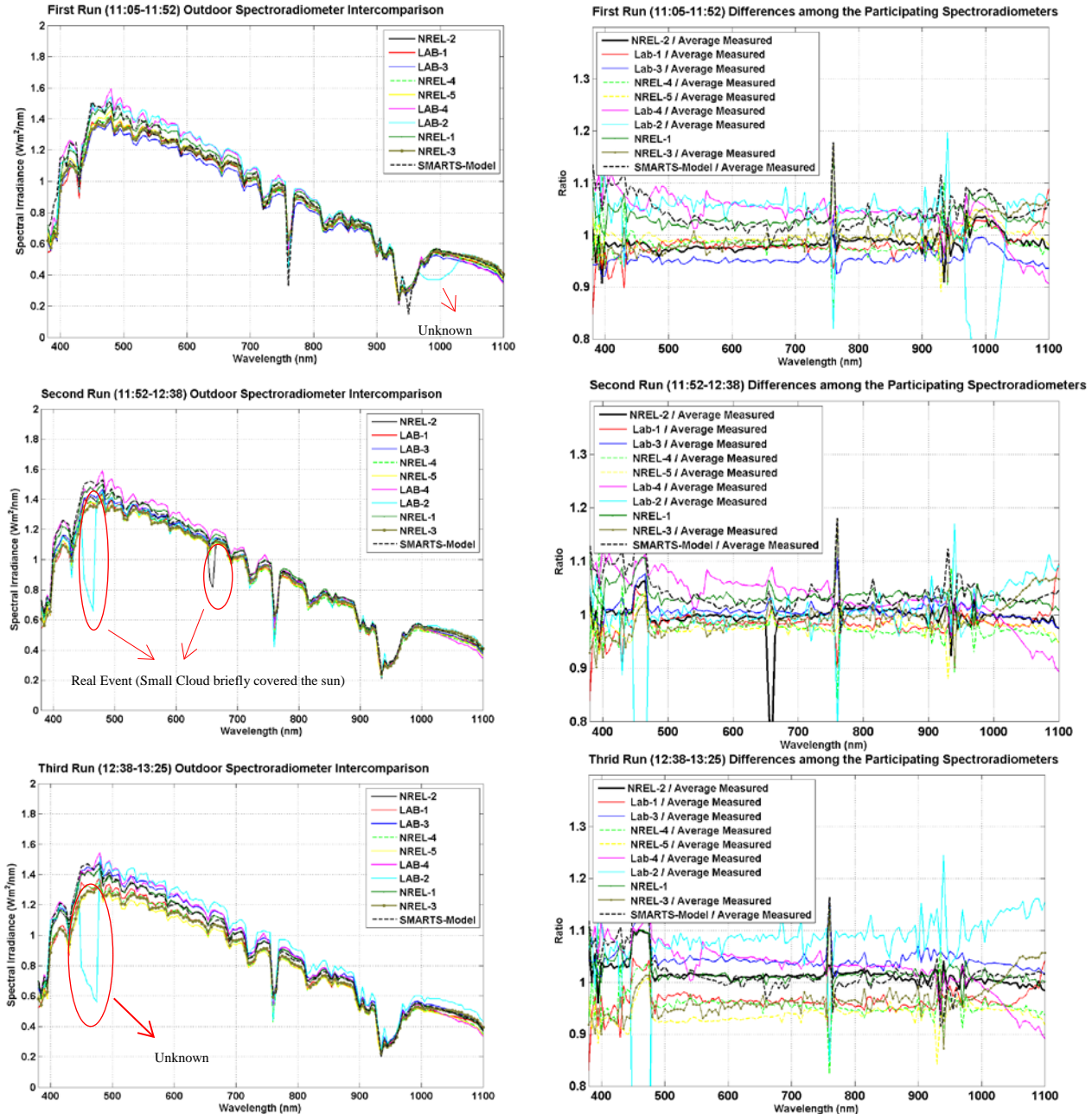


Figure 7. The three outdoor runs, from top to bottom, showing the (left) spectral irradiance plot for each participating spectroradiometer and SMARTS model spectral irradiance output and (right) ratio using the average spectrum from the participating spectroradiometers

4.2.3 Modeled Spectra

In parallel to the outdoor intercomparison itself, a different experiment is discussed in this section to evaluate the additional potential that may be offered by using modeled spectra. This avenue was already explored with success in previous intercomparisons (Martinez-Lozano et al. 2003; Galleano et al. 2013). As in these earlier studies, the SMARTS code (Gueymard 1995, 2001) was retrospectively used to obtain modeled spectra at the time of the measurements.

Comparisons among SMARTS-modeled spectra and actual spectroradiometric measurements at SRRL have been conducted in the past, usually to validate the model itself (Gueymard 2002, 2008, 2011). In the present case, the main intent was to better understand how well the SMARTS-modeled spectra compare to various types of spectroradiometers considering that the model has a finer resolution than the instruments under scrutiny here. Running the smoothing postprocessor of SMARTS was therefore necessary to downgrade the resolution of its spectra and make it match that of any specific instrument based on the shape of its passband (e.g., Gaussian), its width (as measured by the full width at half maximum), and its wavelength step (e.g., 5 nm).

Another aspect to consider when evaluating the potential of using a model such as SMARTS in parallel with spectroradiometric measurements is that scanning instruments (as opposed to solid-state instruments) require more or less significant time to complete their scan during their complete spectral range. In contrast, the model can produce results for any instant during that period. Using repeated simulations (for example, every 5 minutes), it becomes possible to provide useful information about how the actual spectrum changed (at what wavelengths and by how much) during a slow scan. This option, however, requires high-frequency collocated measurements of aerosol optical depth and precipitable water, in particular, because these are the primary—and variable—atmospheric inputs to the model. Such measurements are conducted at only a few laboratories in the world, now including SRRL.

Simulations of global spectral irradiance using SMARTS are shown in Figure 8 for an assumed instrument with a Gaussian 5-nm bandpass and 1-nm wavelength step. These spectra correspond to the mid-times of the three individual runs (11:30 LST, 12:15 LST, and 13:00 LST), yielding air masses of 1.27, 1.27, and 1.32, respectively. The atmospheric conditions did not change much throughout the whole period, so that the spectra at 11:30 LST and 12:15 LST were virtually identical. In the 13:00 LST spectrum, the slight increase in air mass induced an average decrease of approximately 4% in irradiance compared to the two earlier spectra. The SMARTS-modeled broadband global horizontal irradiance values for the three times just mentioned (865.4 W/m^2 , 866.7 W/m^2 , and 827.0 W/m^2 , respectively) closely matched the pyranometer measurements (855.5 W/m^2 , 856.6 W/m^2 , and 831.4 W/m^2 , respectively) from SRRL. The following locally measured information were used to generate these spectra:

- Station pressure (nearly constant): approximately 816 mb
- Total ozone amount (average for that day): 0.281 atm-cm
- Total nitrogen dioxide amount (default value): 0.2 matm-cm
- Precipitable water (measured by SRRL's global positioning system): 1.20 cm to 1.41 cm
- Aerosol optical depth at 500 nm (average of measured value from two sunphotometers at SRRL): 0.06
- Ångström exponent (derived from the direct spectrum measured with a PGS100 instrument located at SRRL): 2.0
- Aerosol single-scattering albedo (derived from sunphotometer data using an inversion method from SRRL): 0.98

- Aerosol asymmetry factor (derived from sunphotometer data using an inversion method from SRRL): 0.71
- Spectral surface reflectance (assumed; selected from the SMARTS library): dry grass

The SMARTS model outputs were used only for corroborative information, and, as previously stated, were not included in the average or difference calculations.

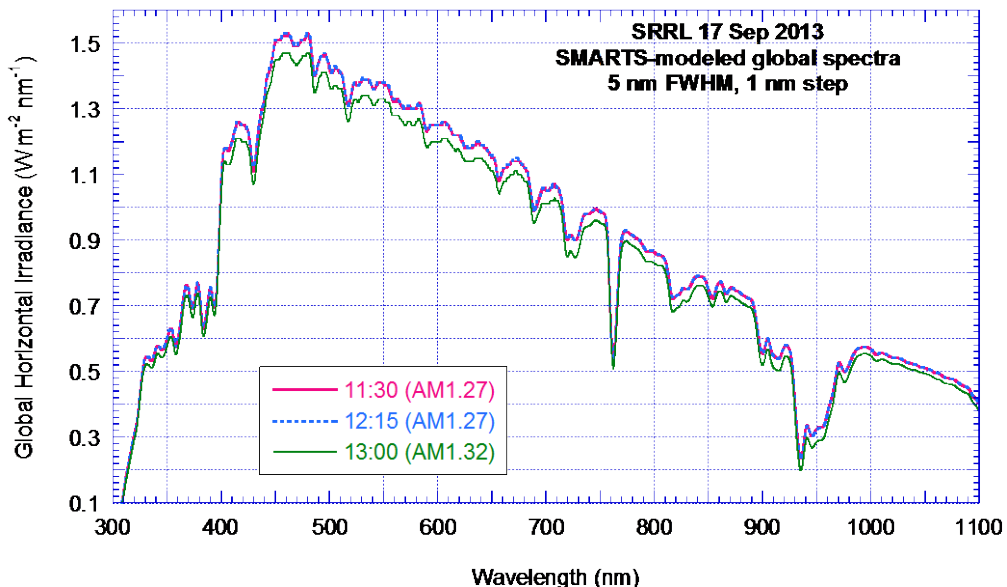


Figure 8. Three spectral irradiance results using the SMARTS model. Input values were selected using the applicable period of run.

4.2.4 Scanning Speed and Cloud Detection

Measuring the spectral irradiance using spectroradiometers involves scanning times from a few seconds to multiple minutes. Under fast-changing atmospheric conditions, slow scanning instruments could have a problem in correctly detecting any natural temporal variability. This may explain some of the largest differences that are apparent in Figure 7. In the present case, the intercomparison was performed under relatively stable sky conditions, which means that even larger differences could result from intercomparing instruments under more variable conditions.

As mentioned above, a small and fast-moving cloud briefly obscured the sun during one of the outdoor runs. This was detected by some instruments and resulted in distorted spectra, as shown in Figure 6 and Figure 7. Generally speaking, fast spectroradiometers assist in detecting a rapid temporal variation of spectral irradiance due to fast-moving clouds. However, during the intercomparison, not all fast-scanning instruments detected the fast-moving cloud. This could be explained by the location of the scanner in a specific wavelength during the passage of the cloud. For example, if the scanner of the fast instrument was located in the infrared region of the wavelength during the cloud passage, then the change in the measured spectral irradiance would be relatively small and relatively unnoticeable.

4.2.5 Performance Analysis

In this report, we illustrate the comparison results and any presence of systematic (bias) or random (scatter) tendencies in the spectral irradiance measurement from each spectroradiometer relative to the measured spectral irradiance averaged throughout 100-nm wide spectral bands and among all instruments. To perform these calculations, mean bias error (MBE) and root mean square error (RMSE) were calculated. The results are shown in percent MBE and RMSE, and they are relative to the average reading of the hundred-wavelength bins. Further, the MBE and RMSE were averaged for the three outdoor runs, as shown in Table 2.

The percent MBE was calculated using the following equation:

$$MBE(\%) = \left(\frac{1}{n} \sum_{i=1}^n \frac{(x_i - \bar{x})}{\bar{x}} \right) * 100$$

Similarly, the percent RMSE was calculated using:

$$RMSE(\%) = \sqrt{\left(\frac{1}{n} \sum_{i=1}^n \left(\frac{x_i - \bar{x}}{\bar{x}} \right)^2 \right)} * 100$$

where x_i represents values from the spectral irradiance under each bin and \bar{x} represents the average of spectral irradiance within each bin.

Table 2. Average MBE and RMSE in Percent

Bins	Average of All vs. NREL-2		Average of All vs. Lab-1		Average of All vs. Lab-3		Average of All vs. NREL-4		Average of All vs. NREL-5		Average of All vs. Lab-4		Average of All vs. Lab-2		Average of All vs. NREL-1		Average of All vs. NREL-3	
	MBE (%)	RMSE (%)	MBE (%)	RMSE (%)	MBE (%)	RMSE (%)	MBE (%)	RMSE (%)	MBE (%)	RMSE (%)	MBE (%)	RMSE (%)	MBE (%)	RMSE (%)	MBE (%)	RMSE (%)	MBE (%)	RMSE (%)
380–400	-0.75	4.85	-8.18	9.77	-1.18	3.76	0.02	7.85	-3.06	5.37	8.18	8.44	6.10	7.11	4.83	6.06	-5.98	6.31
400–500	1.20	3.60	-2.68	4.57	1.34	5.27	-1.90	3.88	-2.92	3.77	8.65	8.97	-4.85	17.52	4.88	5.55	-3.72	4.49
500–600	-0.57	1.52	-1.92	2.04	-0.05	3.34	-2.47	2.54	-3.79	3.81	5.45	5.81	4.24	4.94	2.24	2.29	-3.12	3.30
600–700	-1.43	3.52	-2.42	2.51	-0.05	3.40	-2.57	2.69	-3.32	3.41	5.11	5.17	4.94	5.42	1.90	2.05	-2.16	2.35
700–800	0.14	1.42	-2.92	3.41	0.13	4.25	-3.76	4.85	-2.79	3.27	3.83	4.01	3.16	6.87	2.97	4.26	-0.77	4.35
800–900	0.23	1.18	-3.02	3.15	0.10	3.29	-3.90	3.92	-2.73	2.96	3.05	3.11	4.76	5.27	2.79	2.88	-1.28	1.85
900–1,000	-0.31	2.60	-1.61	2.44	1.10	3.52	-2.64	4.76	-2.56	4.42	1.77	2.78	2.35	10.19	2.96	3.60	-1.05	3.73
1,000–1,100	-0.41	1.13	-0.96	2.55	-0.63	2.88	-3.06	3.46	-2.31	3.34	-4.55	5.83	5.84	11.04	2.25	2.53	3.82	4.45

Figure 9 and Figure 10 show a visual representation of the Table 2 results. Lab-1 had a larger negative MBE for the 380-nm to 400-nm bin. Lab-4 had a higher MBE, between 380 nm and 500 nm.

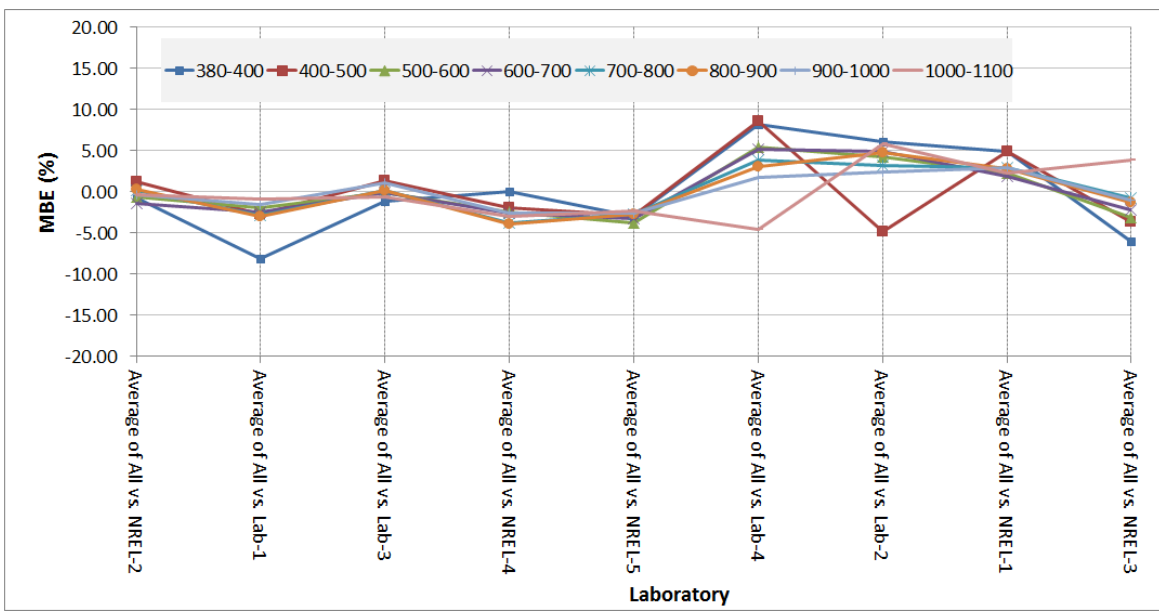


Figure 9. MBE in percent (from Table 2) for various spectral ranges

Lab-2 appeared to have a higher RMSE for the 400-nm to 500-nm range (Figure 10). As described previously, this is likely related to the fast-moving cloud that obscured the sun during the second run and to the unknown experimental condition that occurred during the third outdoor run. Another unknown condition is responsible for the poor performance of Lab-2 in the 900-nm to 1,100-nm range.

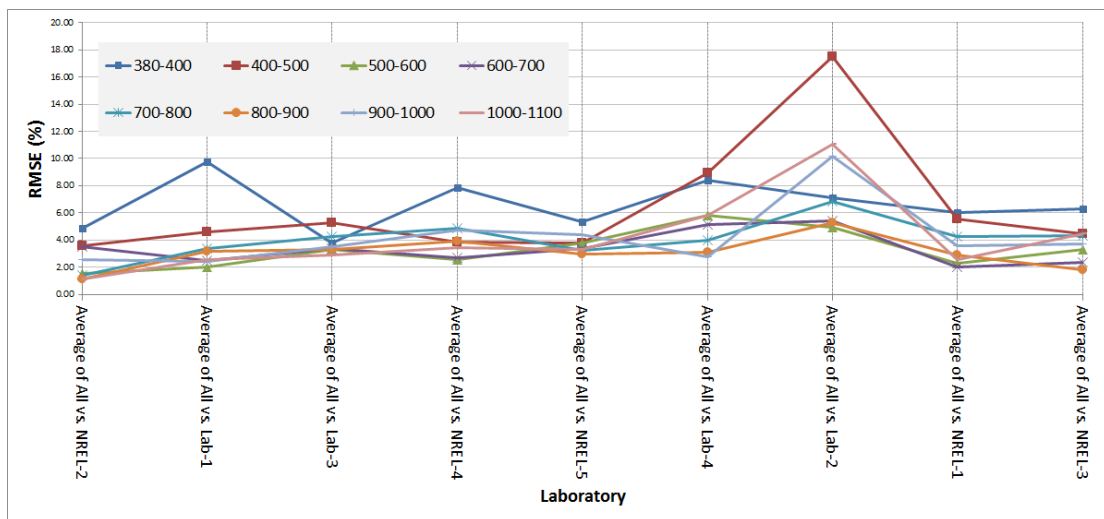


Figure 10. RMSE in percent (from Table 2) for various spectral ranges

However, it is important to note that the differences shown in Table 2, Figure 9, and Figure 10 are average differences from the three outdoor runs and result from the aggregation of hundred-wavelength bins. Because of this averaging of multiple runs and to the spectral aggregation method, relatively low differences were likely obtained because of error cancellations.

4.2.6 Comparison to a Single Instrument

In previous sections, an average of the measured spectral irradiance data was used to determine the differences among spectroradiometers. However, to avoid any bias that might be incurred by using instruments with no temperature controller or instruments with calibration problems—which could eventually affect the averaging of the measured data—in this section, NREL-2 was used as a reference instrument to understand the differences of spectral irradiance data. This does not mean that the NREL-2 is the best instrument among the participating spectroradiometers for outdoor measurements.

Figure 11 shows the ratio obtained by comparing each measured spectral data from the spectroradiometers and the SMARTS model spectral irradiance output to the NREL-2 spectral irradiance data set. Overall, the results showed differences within the $\pm 10\%$ limit. Note, however, that the ultraviolet and infrared regions edged close to this limit.

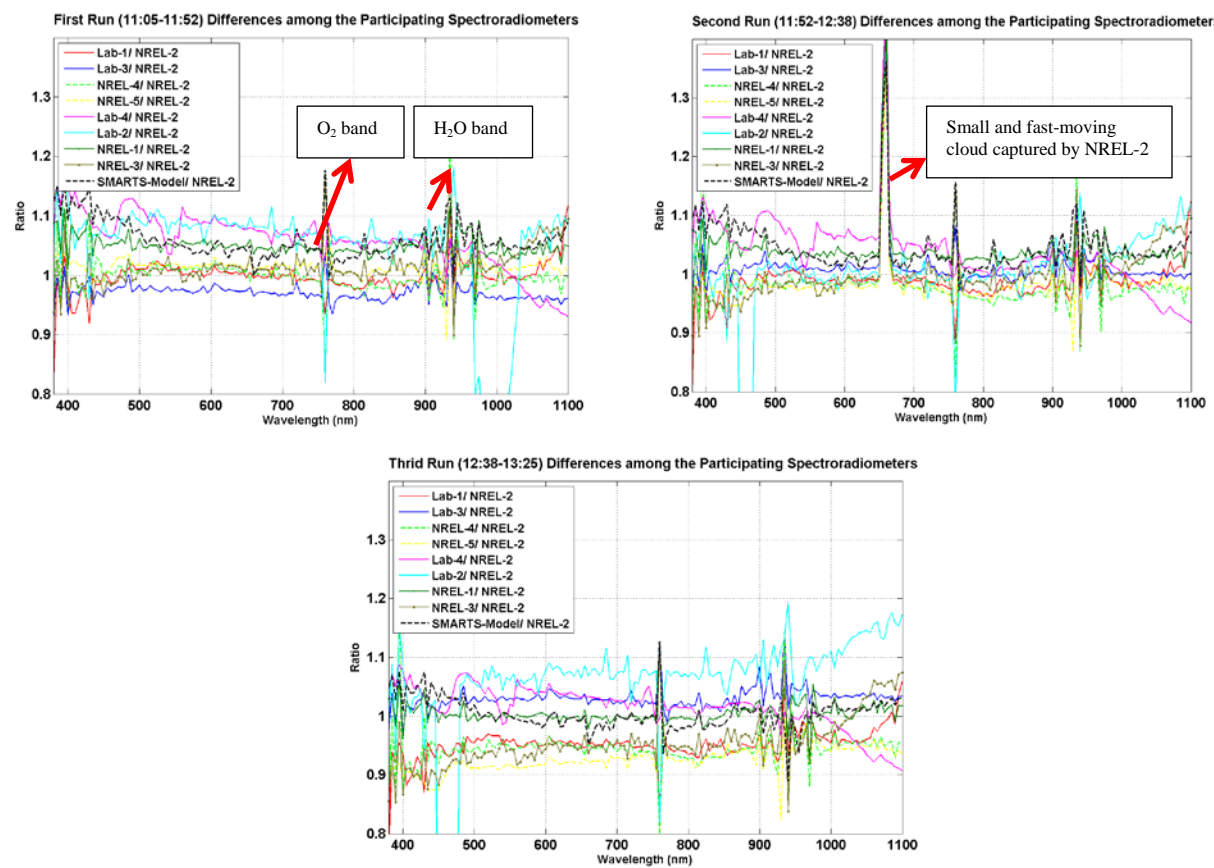


Figure 11. Spectral irradiance data differences for the three runs

5 Summary

The results from the intercomparison exercise described here provide various benefits, such as a better understanding of the performance of the different spectroradiometers under scrutiny, a common platform to compare spectral irradiances under both indoor and outdoor conditions, and the means to verify the technical competence of laboratories. During the event, there were issues related to instrument functions and a few problems related to calibration issues when the calibration file did not work properly with the setting that we used. Some of the problems were solved, and some were not. These types of issues, coupled with the inherent differences in instrument design, calibration methods, and age; source of spectral irradiance calibration lamps; the amount of time since the last calibration of the instrument; incidence angle; reported calibration uncertainty by the laboratories; wavelength shift; environmental conditions; interpolation of data during the analysis; or other experimental issues are the primary reasons for the differences in spectral irradiance measurements in the analysis.

The instruments that participated in the indoor tests demonstrated satisfactory comparisons. The outdoor comparison differences were within $\pm 10\%$, but the ultraviolet and near-infrared spectral bands showed relatively higher differences than the rest of the spectrum. This is explained in part by the usually low performance of most spectroradiometers in the ultraviolet region (a known issue)—unless they are specifically designed to sense ultraviolet wavelengths. Moreover, the spectral irradiance calibration lamps, whether they are NIST primary FEL lamps or secondary lamps, have relatively higher uncertainty in the ultraviolet region due to their low output. Silicon detectors that are not stabilized using temperature controllers usually have low performance in the near-infrared region. This was indeed observed for some of them during the intercomparison. Further, including simulated spectra from the SMARTS model in the outdoor intercomparison provides relevant information when predicting clear-sky solar spectral irradiance under varying atmospheric conditions. The output from the model compares well to the outdoor spectroradiometers spectral irradiance output, and the differences were within the margin of error.

It is anticipated that similar intercomparisons will be held on a regular annual basis in the future and will involve more instruments. The experience gathered during this first event will certainly lead to improved and/or expanded experimental protocols during the preparation of future editions, with the objective to further reduce inter-laboratory differences and uncertainties.

6 References

Cachorro, V.E.; Berjon, A.; Toledano, C.; Mogo, S.; De Frutos, A.M.; Vilaplana, J.M.; Sorribas, M.; De La Morena, B.A.; Gröbner, J.; Laulainen, N. (2009). “Detailed Aerosol Optical Depth Intercomparison between Brewer and Li-Cor 1800 Spectroradiometers and a Cimel Sun Photometer.” *Journal of Atmospheric and Oceanic Technology* (26); pp. 1,558–1,573.

Galleano, R.; Zaaiman, W.; Virtuani A.; Pavanello, D.; Morabito, P.; Minuto, A.; Spena, A.; Bartocci, S.; Fucci, R.; Leanza, G.; Fasanaro, D.; and Catena, M. (2013). “Intercomparison Campaign of Spectroradiometers for a Correct Estimation of Solar Spectral Irradiance: Results and Potential Impact on Photovoltaic Devices Calibration.” *Progress in Photovoltaics: Research and Applications*. Accessed February 2014:
<http://onlinelibrary.wiley.com/doi/10.1002/pip.2361/full>.

Gueymard, C.A. (1995). *SMARTS2: A Simple Model of the Atmospheric Radiative Transfer of Sunshine: Algorithms and Performance Assessment*. FSEC-PF-270-95. Cocoa, Florida: Florida Solar Energy Center. Accessed February 2014:

http://www.solarconsultingservices.com/SMARTS2_report.pdf.

Gueymard, C.A. (2001). “Parameterized Transmittance Model for Direct Beam and Circumsolar Spectral Irradiance.” *Solar Energy* (71); pp. 325–346.

Gueymard, C.A. (2008). “Prediction and Validation of Cloudless Shortwave Solar Spectra Incident on Horizontal, Tilted, or Tracking Surfaces.” *Solar Energy* (82); pp. 260–271.

Gueymard, C.A. (2011). *Validation of Direct Irradiance Spectra Predicted by the SMARTS Radiative Code Using NREL’s Radiometric Data*. Work performed by Solar Consulting Services. Contract No. AGJ-0-40256-01. Golden, CO: National Renewable Energy Laboratory.

Gueymard, C.A.; Myers, D.; Emery, K. (2002). “Proposed Reference Irradiance Spectra for Solar Energy Systems Testing.” *Solar Energy* (73); pp. 443–467.

International Organization for Standards. (1997). ISO/IEC 17043:2010—*Conformity Assessment—General Requirements for Proficiency Testing*. Geneva, Switzerland: International Organization of Standardization.

Lantz, K.; Disterhoft, P.; Early, E.; Thompson, A.; DeLuisi, J.; Kiedron, P.; Harrison, L.; Berndt, J.; Mou, W.; Erhamjian, T.J.; Cabausua, L.; Robertson, J.; Hayes, D.; Slusser, J.; Bigelow, D.; Janson, G.; Beaubian, A.; Beaubian, M. (2002). “The 1997 North American Interagency Intercomparison of Ultraviolet Monitoring Spectroradiometers.” *Journal of Research of NIST (National Institute of Standards and Technology)* (107); pp. 19–62.

Martinez-Lozano, J.A.; Utrillas, M.P.; Pedros, R.; Tena, F.; Diaz, J.P.; Exposito, F.J.; Lorente, J.; De Cabo, X.; Cachorro, V.; Vergaz, R.; and Carreno, V. (2003). “Intercomparison of Spectroradiometers for Global and Direct Solar Irradiance in the Visible Range.” *Journal of Atmospheric and Oceanic Technology* (20); pp. 997–1,010.

Myers, D.R. (1989). “Estimates of Uncertainty for Measured Spectra in the SERI Spectral Solar Radiation Data Base.” *Solar Energy* (43); pp. 347–353.

Thompson, A.; Early, E.A.; DeLuisi, J.J.; Disterhoft, P.; Wardle, D.; Kerr, J.; Rives, J.; Sun, Y.; Lucas, T.; Mestechkina, T.; Neale, P. “The 1994 North American Interagency Intercomparison of Ultraviolet Monitoring Spectroradiometers.” *Journal of Research of NIST (National Institute of Standards and Technology)* (102); pp. 279–322.

Yoon, H.W.; Gibson, C. (2001). *NIST Special Publication 250-89—NIST Measurement Services: Spectral Irradiance Calibration*. Gaithersburg, MD: National Institute of Standards and Technology. Accessed February 2014: <http://www.nist.gov/calibrations/upload/sp250-89.pdf>.